AIAA 2003–3598

Stability of Symmetric and Asymmetric Vortex Pairs over Slender Conical Wing-Body Combinations

Jinsheng Cai, Shijun Luo, and Feng Liu
Department of Mechanical and Aerospace Engineering
University of California, Irvine, CA 92697-3975

33rd AIAA Fluid Dynamics Conference and Exhibit
June 23–26, 2003/Orlando, Florida

Stability of Symmetric and Asymmetric Vortex Pairs over Slender Conical Wing-Body Combinations

Jinsheng Cai*, Shijun Luo†, and Feng Liu‡
Department of Mechanical and Aerospace Engineering
University of California, Irvine, CA 92697-3975

Theoretical analyses are presented for the stability of symmetric and asymmetric vortex pairs over wing-body combinations consisting of a slender circular or elliptic cone and a flat-plate delta wing under small perturbations in an inviscid incompressible steady flow at high angles of attack with or without sideslip. Based on known visualization of experimental high angle-of-attack flows over slender strake-body combinations, one pair of vortices which are separated from the sharp leading edges of the strakes is modeled. The three-dimensional problem of a pair of vortices over the slender conical wing-body combination is reduced to a problem in two-dimensions, for which a general stability condition for vortex pairs can be applied. The stationary positions of symmetric and asymmetric vortex pairs and their stabilities are examined for various geometric configurations, angle of attack, and sideslip. Results are compared with available experimental data and used to shed light on known controversies.

I. Introduction

It is well recognized that the flow over pointed slender bodies becomes asymmetric at high angles of attack. The subject has been studied extensively in relation to air vehicle aerodynamics due to increasing interest in improving maneuverability by extending flight envelopes to higher angles of attack. The subject has been reviewed by Hunt,[1] Ericsson and Reding,[2] and by Champigny.[3]

It is found by numerous experimental studies[4,5] and numerical results[6–8] that micro-asymmetric perturbations close to the nose tip produces a strong flow asymmetry. There seems little doubt that the vortex asymmetry is triggered, formed, and developed in the apex region, and the after portion of the forebody and the after cylindrical body (if any) have little effect on the asymmetry over the apex region. The perturbation evolution at the apex plays an important role in determining the flow pattern over the entire body.

Since the apex portion of any slender pointed body is nearly a conical body, high angle-of-attack flow about conical bodies has been studied extensively. Dyer, Fiddes and Smith[9] calculated symmetric and asymmetric vortex flows over circular cones, and predicted that the asymmetry onset angle-of attack is about twice of the semi-vertex angle, which agrees well with known experimental observations. Pidd and Smith[10] studied a spatial, or otherwise called convective, type of instability of the symmetric and asymmetric vortices found by Dyer et al.[9]

Huang and Chow[11] used a simplified vortex model and succeeded in showing by an analytical method that the vortex pair over a slender flat-plate delta wing at zero sideslip can be stationary and is stable under small conical perturbations , which agreed with the experimental results of Stahl, Mahmood and Asghar.[12]

The present authors[13] developed a general stability condition for vortices in a two-dimensional incompressible inviscid flow field. A mathematical framework was presented to reduce the problem of a three-dimensional potential flow over slender conical bodies at high angles of attack to the solution of a two-dimensional problem. The two-dimensional stability condition was then extended to analyze the absolute (temporal) stability of symmetric vortex pairs over three-dimensional slender conical bodies. The bodies considered include circular cones and highly swept flat-plate wings with and without vertical fins, and elliptic cones of various eccentricities. Results based on the theory agreed well with known experimental observations.

The present authors extended their previous analysis[13] to include asymmetric vortices over slender conical bodies in Ref. 14, and predicted that the stationary asymmetric vortex pairs over circular cone at high angles of attack with symmetric and asymmetric separations are unstable under small perturbations. The

*Visiting Associate Researcher. Currently Research Scientist, Temasek Laboratories, National University of Singapore. Member AIAA.
†Researcher.
‡Associate Professor. Senior Member AIAA.

above prediction agreed with the experimental observations of Jenista and Nelson[15] and the experimental interpretation of Ericsson and Reding.[2] However, it did not agree with experimental and analytical results reported by Lowson and Ponton[16] and Pidd and Smith,[10] where they noted observations of stable conical symmetric and asymmetric vortices over a circular cone.

In the scenario of a convective instability, the originally undisturbed stationary symmetric and asymmetric vortices were conical. However, the spatially disturbed vortices were no longer conical. Pidd and Smith[10] were able to perform analysis of this type of instability by using the slender-body theory.

The type of instability studied in Refs. 13 and 14 refers to a temporal evolution of the conical symmetric or asymmetric vortices. The flow stays conical before or after the disturbance. However, the disturbances are of a 'global' nature. Satisfaction of this 'absolute' type of stability condition should be regarded as one necessary condition for any configuration of a conical symmetric or asymmetric vortex pattern to persist in a flow.

Because of the undesirable effects associated with the forebody flow asymmetries, numerous means of alleviating the problem have been devised. Most of them work in the apex region. One of the devices is the nose strakes. Coe, Chambers and Letko[17] showed by wind tunnel tests alleviating effects of horizontal and symmetrical strakes placed close to the apex of a slender ogive forebody and a circular cone. Champigny[3] showed in his figure 29 that when the narrow wings are located very far forward on the pointed-nose body of an ONERA-S3MA model, the side forces at high angles of attack are substantially reduced. It was shown by water tunnel visualization that the symmetric forebody vortices developed on an F-18-type configuration at high angle of attack and zero sideslip are strongly entrained on to the wing by the powerful vortices shed from the wing leading-edge extensions.[18] Nelson et al.[19] gave in their figure 32 the smoke/laser sheet and fluorescent minituft photograph of the surface and wake flow around a high performance aircraft model at a 20-deg angle of attack, and in Plate 1 the wake image survey of the same flow. It is interesting to study the stability characteristics of the separation vortex flow over slender conical wing-body combinations at high angles of attack by analytical methods.

In this paper, we extend our previous analysis in Ref. 14 to include symmetric and asymmetric vortices over slender conical wing-body combinations. The vortex model used for wing-body combination is first established. The analytical methods are briefly reviewed. The stability of stationary symmetric and asymmetric vortex flows over slender flat-plate delta wing and circular or elliptic cone combinations with and without sideslip are analyzed in detail by the present theory. Comparisons are made with available experimental observations. Results help clarify certain experimental controversies.

II. Vortex Model for Wing-Body Combinations

It is known that for an isolated slender body such as a circular cone, an elliptic cone or a flat-plate delta wing at high angles of attack, there appears one pair of separation vortices starting from the apex of the body. In the case of wing-body combination, Coe, Chambers & Letko[17] (1972) investigated experimentally the effectiveness of flat-plate strakes placed symmetrically and horizontally on the nose of a circular cone and a tangent-ogive body of revolution. A tuft grid was placed slightly behind the models to visualize the flow fields. The experimental Reynolds number is about 0.2×10^6 based on the maximum body diameter. The result was evidenced by their figure 25 which gave the tuft grid photographs for a pointed-tip tangent-ogive model of fineness ratio of 3.5 with strakes and a blunt-tip paraboloid of revolution with the same fineness ratio at angles of attack of 30 and 55 degrees and zero sideslip. It is seen that the flow field behind the ogive-strake model is very similar to the flow field behind the paraboloid of revolution. Only one pair of separation vortices was observed over the ogive-strake combination. It is noted that the effect of the strakes was to produce well-defined points of separation which resulted in one symmetrical vortex pair over the entire wing-body combination at high angles of attack.

Nelson and Malcolm[19] (1992) gave in their figure 32 the photographs of smoke/laser sheet of the flow field and fluorescent minituft on the body surface around a high performance aircraft model at an angle of attack of 20 degrees, obtained by J.P. Crowder of the Boeing Aerodynamics Laboratory (1985 unpublished). In this case, the strakes are the leading-edge extensions of the main wing. The photographs showed that a pair of vortices was separated from the leading edges of the strakes, and no other vortices were found in the flow field of the strake-body station. The fluorescent minitufts showed the strong spanwise flow on the upper surfaces of the strakes and fuselage created by the vortex pair. Crowder also used the wake imaging system to determine the total pressure field for the same model. Plate 1 of ref. 19, a color-coded total pressure survey, showed also one pair of vortices separated from the strake leading edges in the flow field of the strake-fuselage station at angle of attack of 20 degrees.

In fact, since the strakes are much thinner than the fuselage, the flow first separates from the sharp leading edges of the strakes as the angle of attack begins

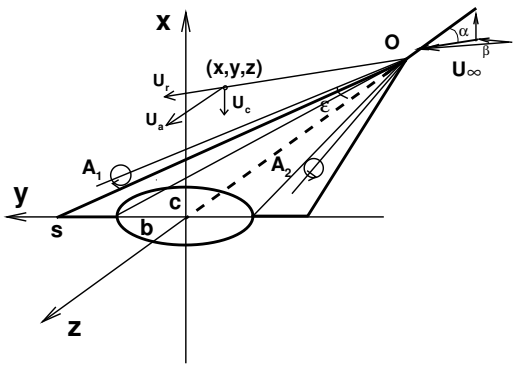

Fig. 1 Slender conical wing-body combination and separation vortices.

to increase from zero. Once the strake vortex pair is formed, it grows and dominates the flow field. Based on these experimental observations, the vortex model chosen for the present analytic study of the separation flows over conical slender wing-body combinations is one pair of concentrated vortices separated from the leading edge of the flat-plate wing, OA_1 and OA_2 as shown in Fig.1. The distributed vortex sheets that connect the leading edges and the two concentrated vortices are neglected since their strength is in general much smaller than that of the two concentrated vortices. The two concentrated vortices are assumed to be rays from the body apex O under conical flow assumption. Secondary separation vortices, if any, are weak, and also neglected.

III. Governing Equations and Analytic Methods

The reader is referred to Ref. 13 for details of the theoretical background. The following subsections only serve to summarize the necessary equations for the wing-body combinations under present consideration.

A. Positions and Strengths of Stationary Vortices

Consider the flow past a slender conical wing-body combination at an angle of attack α and sideslip angle β as shown in Fig. 1. The velocity of the free stream flow is U_∞. The combination has a slender triangular flat-plate wing passing through the longitudinal axis of the body. The flow separates from the wing sharp leading edge and the flow is assumed to be steady, inviscid, incompressible, conical, and slender.

The inviscid incompressible flow considered in the above model is irrotational except at the centers (cores) of the isolated vortices. The governing equation for the velocity potential is the three-dimensional Laplace equation with zero normal flow velocity on smooth body surfaces, and Kutta conditions at sharp edges as boundary conditions. By the principle of superposition, the flow around the body can be obtained by solving the following two flow problems: (1) the flow due to the normal components of the freestream velocity, $U_x = U_\infty cos\beta sin\alpha$ and $U_y = U_\infty sin\beta$; and (2) the flow due to the axial component of the freestream velocity, $U_a = U_\infty cos\beta cos\alpha$, both subject to the boundary conditions.

Under the assumption of conical and slender flow, the three-dimensional flow problem is reduced to a two-dimensional flow problem. The flow in each cross section at z may then be regarded as a two-dimensional flow across the local cross sectional profile governed by the two-dimensional Laplace equation with the boundary conditions. Solution to this two-dimensional velocity field is obtained by conformal mapping or other analytical or numerical methods and by the condition of conical flow in which the flow is invariant along rays emanating from the apex. For simple profiles such as a wing-elliptic body combination, the conformal mapping for this profile in the plane $Z = x + iy$ to a circle of radius r in a uniform flow of velocity $(U_x/2, U_y/2)$ in the plane $\zeta = \xi + i\eta$ is,

$$Z = \frac{1}{2}\left(\phi + \frac{\lambda}{\phi}\right), \quad \phi = \varphi + \sqrt{\varphi^2 + 1}, \quad \varphi = \frac{1}{2}\left(\zeta - \frac{r^2}{\zeta}\right)$$

where $c = \frac{1+\lambda}{2}$ and $b = \frac{1-\lambda}{2}$ are the semi-axes of the ellipse along the x and y axes, $r = [bs - c\sqrt{s^2 + 2c - 1}]/(1 - 2c)$, and s is the semi-span of the flat plate, and the overbar denotes complex conjugate.

The complex velocity on the cross-flow plane Oxy is,

$$\begin{aligned} u - iv &= \left[\frac{1}{2}\left(\overline{U_n} - \frac{U_n r^2}{\zeta^2}\right)\right. \\ &+ \frac{i\Gamma_1}{2\pi}\left(\frac{1}{\zeta - \zeta_1} - \frac{1}{\zeta - r^2/\overline{\zeta_1}}\right) \\ &- \left.\frac{i\Gamma_2}{2\pi}\left(\frac{1}{\zeta - \zeta_2} - \frac{1}{\zeta - r^2/\overline{\zeta_2}}\right)\right]\left(\frac{d\zeta}{dZ}\right) \\ &- \frac{U_x \overline{Z}}{sK} + \frac{1}{2\pi}\sum_{j=1}^{N}\frac{Q_j}{Z - Z_j} \end{aligned} \tag{1}$$

where the overbar denotes complex conjugate; $U_n = U_x(1 + iK_S)$; $K_S = \tan\beta/\sin\alpha$ is the sideslip similarity parameter; $K = \frac{tan\alpha}{tan\epsilon}$ is the Sychev similarity parameter (Sychev[20]); ζ_1 and ζ_2, and Γ_1 and Γ_2 are the positions and strengths of the vortex 1 and vortex 2, respectively; Q_j is the strength of the point sources at Z_j and $Q_j (j = 1, 2, ...N)$ are to be determined by N simultaneous equations of the boundary condition on the body contour.

The complex velocity at the vortex point Z_1 (or ζ_1) is obtained by a limiting process (see Rossow[21]).

$$\begin{aligned} u_1 - iv_1 &= \left[\frac{1}{2}\left(\overline{U_n} - \frac{U_n r^2}{\zeta_1^2}\right) + \frac{i\Gamma_1}{2\pi}\left(-\frac{1}{\zeta_1 - r^2/\overline{\zeta_1}}\right)\right. \\ &- \left.\frac{i\Gamma_2}{2\pi}\left(\frac{1}{\zeta_1 - \zeta_2} - \frac{1}{\zeta_1 - r^2/\overline{\zeta_2}}\right)\right]\left(\frac{d\zeta}{dZ}\right)_1 \\ &- \frac{i\Gamma_1}{4\pi}\left(\frac{d^2Z}{d\zeta^2}\right)_1\left(\frac{d\zeta}{dZ}\right)_1^2 \\ &- \frac{U_x\overline{Z_1}}{sK} + \frac{1}{2\pi}\sum_{j=1}^{N}\frac{Q_j}{Z_1 - Z_j} \end{aligned} \tag{2}$$

where the subscript 1 denotes the values at $Z = Z_1$ (or $\zeta = \zeta_1$). A similar expression is obtained for the complex velocity, $u_2 - iv_2$ at the vortex point Z_2 (or ζ_2).

The stationary positions, Z_1 (or ζ_1) and Z_2 (or ζ_2), and strengths of the vortices, Γ_1 and Γ_2, are determined by solving a set of algebraic equations. These are $u_1 - iv_1 = 0$ and $u_2 - iv_2 = 0$ for the vortex velocity fields, and two more equations that set the flow velocities to be finite values at the sharp edges of the flat plate (Kutta condition). The four algebraic equations are linear in Γ_1 and Γ_2, and non-linear in Z_1 (or ζ_1) and Z_2 (or ζ_2). They are solved by an iteration method. A Newton iteration for the vortex locations is constructed for $\mathbf{F}(\mathbf{X}) = 0$, where $\mathbf{F} = [u_1, v_1, u_2, v_2]^T$, $\mathbf{X} = [\xi_1, \eta_1, \xi_2, \eta_2]^T$, $\zeta_1 = \xi_1 + i\eta_1$, and $\zeta_2 = \xi_2 + i\eta_2$. Given the vortex positions ζ_1 and ζ_2, the vortex strengths Γ_1 and Γ_2 can be obtained by using the separation conditions.

B. Stability of the Stationary Vortices

When a vortex is slightly perturbed from its stationary position, the increments of its coordinates as function of time are governed by a system of linear homogeneous first-order ordinary differential equations as shown in Ref. 13. The perturbations can be decomposed into a symmetric perturbation $Z_1 = Z_{10} + \Delta Z$, $Z_2 = Z_{20} + \overline{\Delta Z}$ and an anti-symmetric perturbation $Z_1 = Z_{10} + \Delta Z$, $Z_2 = Z_{20} - \overline{\Delta Z}$ where $\Delta Z = \Delta x + i\Delta y$, $|\Delta x| \ll s$, and $|\Delta y| \ll s$. The eigenvalues of the coefficient matrix in the dynamic equations are λ_1 and λ_2. Define the Jacobian and divergence of the vortex velocity field $\mathbf{q} = (u, v)$,

$$J = \begin{vmatrix} \frac{\partial u}{\partial x} & \frac{\partial u}{\partial y} \\ \frac{\partial v}{\partial x} & \frac{\partial v}{\partial y} \end{vmatrix}, \quad D = \nabla \cdot \mathbf{q} = \frac{\partial u}{\partial x} + \frac{\partial v}{\partial y} \tag{3}$$

It can be easily shown that the eigenvalues of this problem are

$$\lambda_{1,2} = \frac{1}{2}\left(D_0 \pm \sqrt{D_0^2 - 4J_0}\right) \tag{4}$$

where the subscript 0 denotes values at (x_0, y_0). The maximum real part of the two eigenvalues λ_1 and λ_2 in Eqn. (4) will be plotted and used to determine stability in this paper. A positive value of this variable means instability of the vortex system.

IV. Analysis of Typical Model Configurations

This section discusses the application of the above analytical methods to a number of wing-body combinations typical of aeronautical applications.

To comprehend the analytic results obtained below for the wing-body combinations, it is useful to review the vortex flow characteristics of isolated wing and isolated body obtained in the previous papers[13,14] by the present authors.

1. For slender flat-plate delta wing at high angles of attack, the stationary leading-edge separation vortices are stable under any small perturbations, and there exist no stationary asymmetric vortices if the wing has no sideslip.

2. For slender circular cone at high angles of attack, the stationary symmetric vortex pair is unstable under small perturbations, and there exists a stationary asymmetric vortex pair when the angle of attack is large enough and even when the separation lines are prescribed to be symmetric. The stationary asymmetric vortex pair is also unstable under small perturbations no matter the separation lines are symmetric or asymmetric. Thus, vortex flow over circular cones cannot be conical.

3. For slender elliptic cones at high angles of attack, as its thickness ratio decreases from 1 (circular cone) to 0 (flat-plate delta wing), the vortex flow characteristics changes gradually from that of a circular cone to that of a flat-plate delta wing.

A. Flat-Plate Delta Wing and Circular-Cone Combination

Consider a wing-body combination of a flat-plate delta wing and a circular-cone body with a body thickness to wing span ratio $\gamma = a/s = 0.7$ at zero sideslip, i.e., $K_S = 0$. As a general approach, stationary symmetric and asymmetric vortex locations are found and shown to illustrate the possible conical vortex patterns for a range of parameters. Then, the stability of the stationary vortices is examined by looking at the eigenvalues of the vortex system as given by Eqn. (4) and calculated at their stationary positions. Fig. 2 shows the calculated location of stationary symmetric and asymmetric vortex pairs for K ranging from 2 to 4.5. Within this range of K, either a stationary symmetric vortex pair or a stationary asymmetric vortex pair may

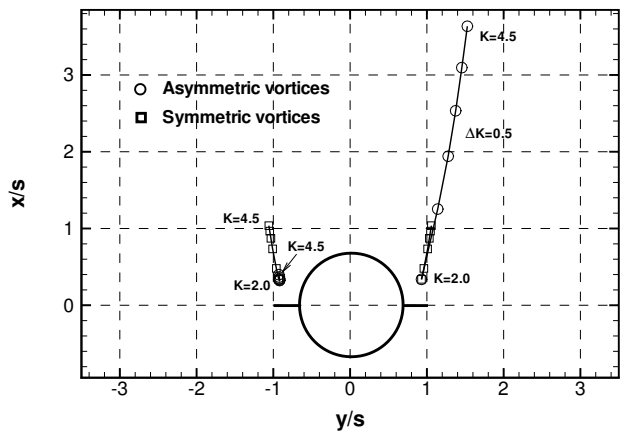

Fig. 2 Location of stationary symmetric and asymmetric vortex pairs over a wing-body combination of a flat-plate delta wing and a circular-cone body, $\gamma = a/s = 0.7$, $K = 2 \sim 4.5$, $K_S = 0$.

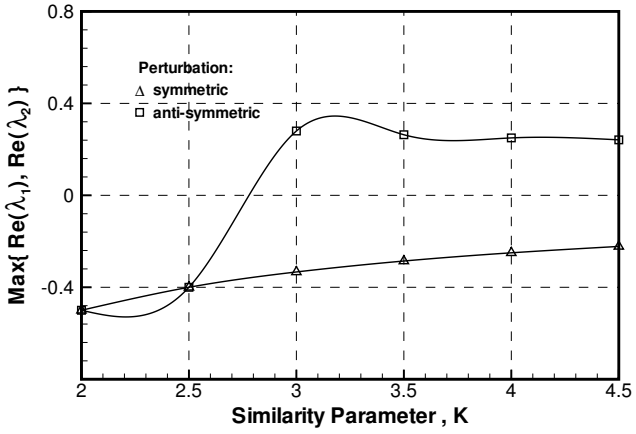

Fig. 3 Maximum real part of the eigenvalues for symmetric vortex pairs over a wing-body combination of a flat-plate delta wing and a circular-cone body, $\gamma = a/s = 0.7$, $K = 2 \sim 4.5$, $K_S = 0$.

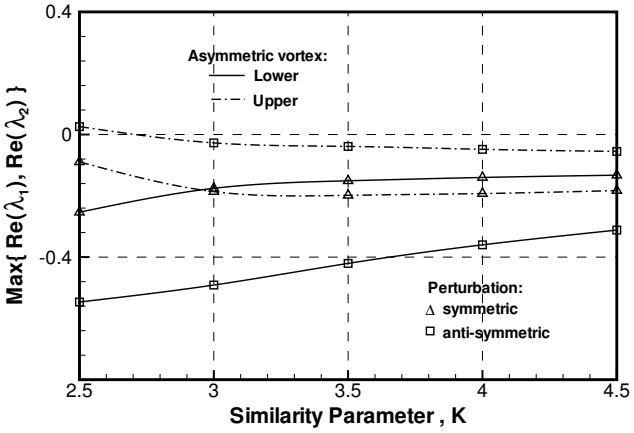

Fig. 4 Maximum real part of the eigenvalues for asymmetric vortex pairs over a wing-body combination of a flat-plate delta wing and a circular-cone body, $\gamma = a/s = 0.7$, $K = 2.5 \sim 4.5$, $K_S = 0$.

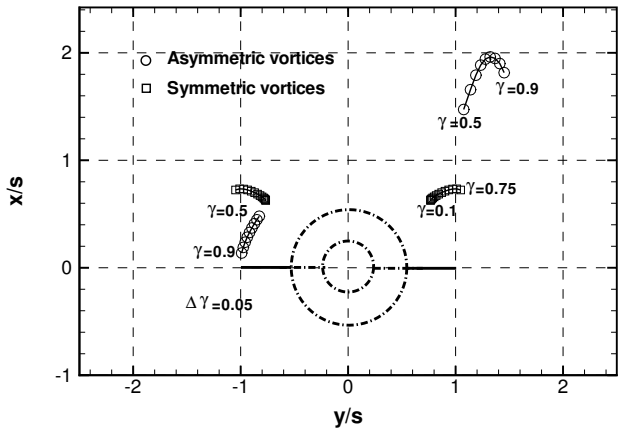

Fig. 5 Location of stationary symmetric and asymmetric vortex pairs over a wing-body combination of a flat-plate delta wing and a circular-cone body, $\gamma = a/s = 0.1 \sim 0.9$, $K = 3$, $K_S = 0$.

exist for the same K. However, no stationary asymmetric vortex pair is found in the computation when $K \leq 1.5$. As K is increased, i.e., when the flow angle of attack is increased for the given geometry, both the symmetric and asymmetric vortex pairs move upward and outboard. The movement of the lower vortex of the asymmetric vortex pair is much smaller and that of the upper vortex is much larger compared to movements of the symmetric vortices.

Fig. 3 shows the eigenvalues vs. K for the symmetric vortex pair (only the maximum real part of the two eigenvalues are plotted here and in other figures.) The symmetric vortex pair is stable when $K \leq 2.8$ and unstable otherwise. Fig. 4 shows the eigenvalues for the asymmetric vortex pair. In the calculated region of K, the lower vortex is stable while the upper vortex is only stable when $K > 2.7$. The upper vortex is more unstable than the lower one under anti-symmetric disturbances. It is interesting to note for this case that as a whole the symmetric pair is stable when $K \leq 2.8$ while the asymmetric pair becomes stable when $K \geq 2.7$. This indicates that an initially symmetric vortex pair at low angles of attack is likely to transit to an asymmetric pair when the angle of attack is increased to levels beyond $K = 2.7 \sim 2.8$.

To study the effect of the body-thickness-to-wingspan ratio $\gamma = a/s$, we examine the case with a fixed $K = 3$ and no sideslip ($K_S = 0$). Fig. 5 shows the

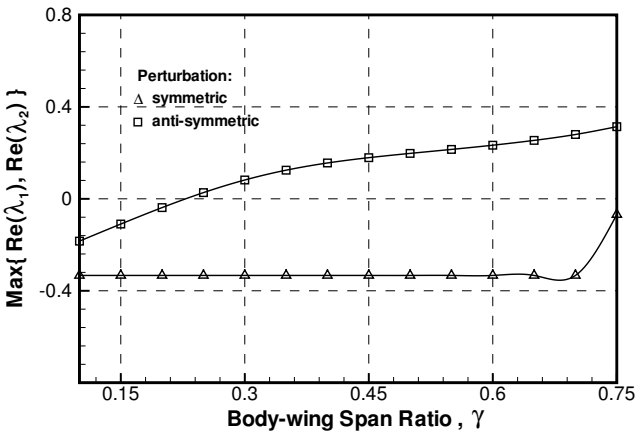

Fig. 6 Maximum real part of the eigenvalues for symmetric vortex pairs over a wing-body combination of a flat-plate delta wing and a circular-cone body, $\gamma = a/s = 0.1 \sim 0.75$, $K = 3$, $K_S = 0$.

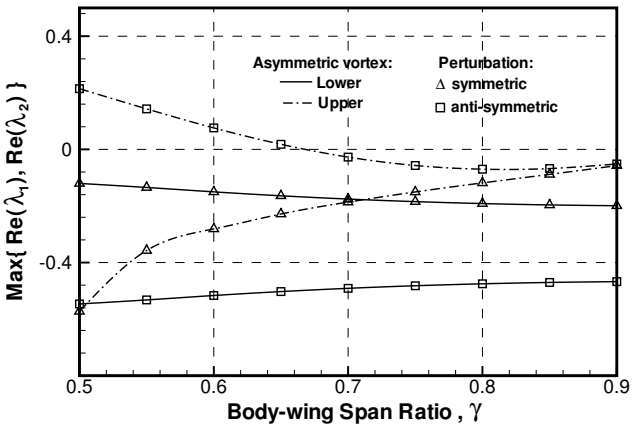

Fig. 7 Maximum real part of the eigenvalues for asymmetric vortex pairs over a wing-body combination of a flat-plate delta wing and a circular-cone body, $\gamma = a/s = 0.5 \sim 0.9$, $K = 3$, $K_S = 0$.

computed location of stationary symmetric and asymmetric vortex pairs for $\gamma = a/s$ ranging from 0.1 to 0.9. When the body-wing span ratio $\gamma \leq 0.50$, no stationary asymmetric vortex pairs can been found. When $\gamma \geq 0.5$ both the symmetric and the asymmetric configurations are possible. When γ increases both vortex pairs move outboard, and the lower vortex of the asymmetric vortex pair goes downward toward the wing leading edge and the upper vortex goes upward first and then downward.

Fig. 6 shows the eigenvalues of the symmetric vortex system vs. γ. Increase of the size of the center circular cone relative to the wing span destabilizes the symmetric vortices. The symmetric vortex pair is only stable when $\gamma \leq 0.23$ and becomes unstable when $\gamma > 0.23$. Notice that no stationary asymmetric vortex pair can be found, as pointed out earlier, even though the stationary symmetric vortex pair is unstable for $0.23 < \gamma < 0.50$. This indicates that the instability of a stationary symmetric vortex pair does not necessarily bring about the existence of a stationary asymmetric vortex pair under the same conditions.

Fig. 7 shows the eigenvalues of the asymmetric vortex pair versus γ. The upper vortex is more unstable than the lower one under anti-symmetric perturbations. The lower vortex is stable for all $0.5 \leq \gamma \leq 0.9$ calculated, while the upper vortex is only stable when $\gamma \geq 0.66$. Thus, the asymmetric vortex pair as a whole is stable when $0.66 \leq \gamma \leq 0.9$. It is noted that in the calculated range of γ ($0.5 \sim 0.9$), both the symmetric and the asymmetric vortex pairs are unstable when $0.23 < \gamma < 0.66$. This implies that the vortex flow cannot be conical under this condition.

Coe et al.[17] placed a pair of small strakes near the tip of a circular cone in their experiments to suppress vortex asymmetry. The circular cone had a fineness ratio, $L/D = 3.5$, where L and D are the length and the base diameter of the cone, respectively, resulting a semi-vertex angle of 8.13 degrees for the cone. A pair of flat-plate strakes are placed on the nose of the cone. The planform of the small strake is rectangular, $0.0833D$ wide by $0.583D$ long. The leading edge of the strakes is placed at $x = 0.0476L$ after the nose tip. The experimental Reynolds number is 0.35×10^6. They showed that the strakes significantly reduced the originally large asymmetric forces as the angle of attack varied from 0 to 75 degrees at zero sideslip (figure 24(b) in Ref.[17]). Although no strict equivalent configuration of the present conical wing-body combination of a circular cone and a flat-plate delta wing can be made to the above experimental setup, a rough approximation is made by using a strake of conical planform whose leading edges pass through the two front corners of the rectangular strakes in Coe et al.[17] since the separation vortices must start from these corner points. This leads to a semi-apex angle, ϵ, of 30 degrees, resulting in a γ of close to 0.25. According to Fig. 6 of the present theory, the symmetric vortex pair over the experimental model is stable for K up to 3, which means $\alpha = 60°$. The theoretical analysis is consistent with the experimental observations of Coe et al..[17] By placing a pair of horizontal strakes near a pointed body nose, the original separation lines move from the smooth body surface to the sharp edges of the strakes. If the strakes are wide enough, the vortex-flow characteristics changes from that of pointed body of revolution to that of sharp-edge delta wing, which tend to stabilize the symmetric vortex pair.

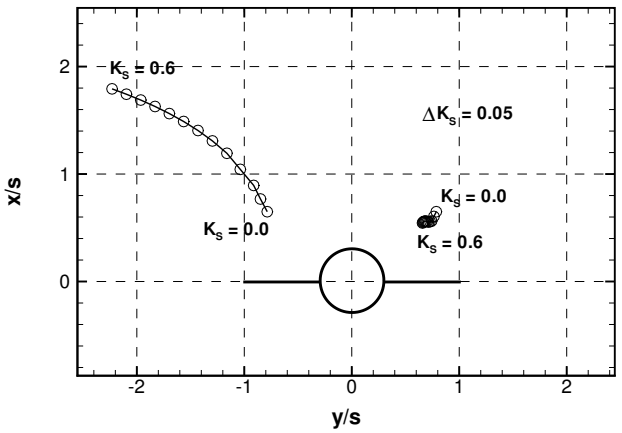

Fig. 8 Location of stationary vortex pairs over a wing-body combination of a flat-plate delta wing and a circular-cone body, $\gamma = a/s = 0.3$, $K = 3$, $K_S = 0 \sim 0.6$.

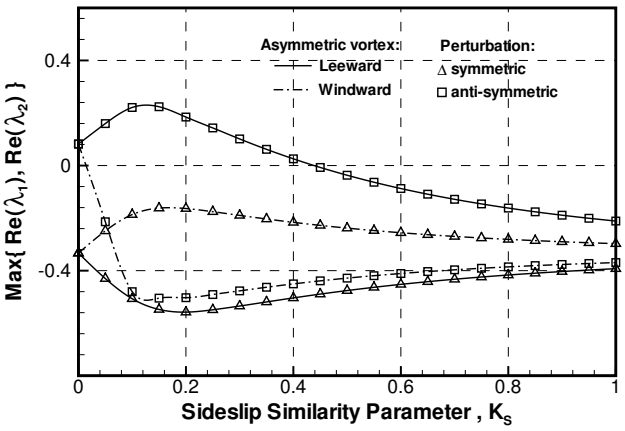

Fig. 9 Maximum real part of the eigenvalues for asymmetric vortex pairs over a wing-body combination of a flat-plate delta wing and a circular-cone body, $\gamma = a/s = 0.3$, $K = 3$, $K_S = 0 \sim 1$.

It is known that placing a triangular flat-plate fin of enough height near the tip of pointed body in the leeward incidence plane can also reduce the vortex asymmetry at high angles of attack as shown by the experiments of Asghar, Stahl & Mahmood[22] and Ng,[23] and confirmed with the analytical results of the present authors in Ref. 13. Furthermore, it is shown in Ref. 13, that when the separation lines occur on the windward side of circular cone, both leeward and windward fins in the incidence plane are needed to suppress the vortex asymmetry. It is noted that the vertical fins work with a different mechanism of suppressing the vortex asymmetry from that of the horizontal strakes. The vertical fins suppress the vortex asymmetry by hindering the interaction between the symmetric vortex pair at high angles of attack, while the horizontal strakes suppress the vortex asymmetry by forcing the separation line to the edge of the strakes and stretching the two symmetric concentrated vortices away from each other to reduce the interaction between the two vortices.

Finally, we study the situation with sideslips for a wing-body combination with $\gamma = a/s = 0.3$ and $K = 3$. There are no stationary symmetric vortex pairs under non-zero sideslip. Fig. 8 shows the possible stationary asymmetric vortex pairs for the sideslip similarity parameter K_S to range from 0.0 to 0.6. When the sideslip similarity parameter K_S increases the windward vortex goes slightly inboard and downward, and the leeward vortex stretches significantly outboard and upward.

Fig. 9 shows the maximum real part of the two eigenvalues versus the sideslip similarity parameter K_S. The windward vortex is unstable when $K_S < 0.016$ and stable when $K_S > 0.016$. The leeward vortex is unstable when $K_S < 0.433$ and stable when $K_S > 0.433$. From Fig. 6 one can find when $K_S = 0$, $\gamma = a/s = 0.3$ and $K = 3$ the stationary symmetric vortex pair is not stable, and from Fig. 9 one can find the stationary asymmetric vortex pair is stable when $K_S > 0.433$. This means that the sideslip can make the originally unstable symmetric vortex pair at zero sideslip to become stable and asymmetric. It is seen that for the considered asymmetric vortices under anti-symmetric disturbances, the leeside (upper) vortex is more unstable than the wind-side (lower) vortex.

B. Flat-Plate Delta Wing and Elliptic-Cone Combination

Consider the case when the body-span-to-wing-span ratio $\gamma = b/s = 0.7$ and the thickness to span ratio of elliptic body $\tau = c/b = 1.5$ with zero sideslip ($K_S = 0$). Fig. 10 shows the location of possible stationary symmetric vortex pairs vs. K in the range from 1.0 to 8.0. The symmetric vortex pair first appear near the upper surface of the wing and moves upward and outboard as K increased from 1. The vortex movement is extraordinarily large when K is increased from 4 to 5, and when $K \geq 5.0$ the symmetric vortex pair is located higher than the uppermost point of the body. No stationary asymmetric vortex solutions are found when $K \leq 4.66$.

Fig. 11 shows the eigenvalues of the symmetric vortex pair vs. K. The symmetric vortex pair is stable when $K < 4.5$ and unstable when $K > 4.5$. It is interesting to note that this transition happens right between $K = 4$ and $K = 5$ when the symmetric vortex pair is moving abruptly away from the the wing to over the body top.

Consider a case with a high body thickness-to-span

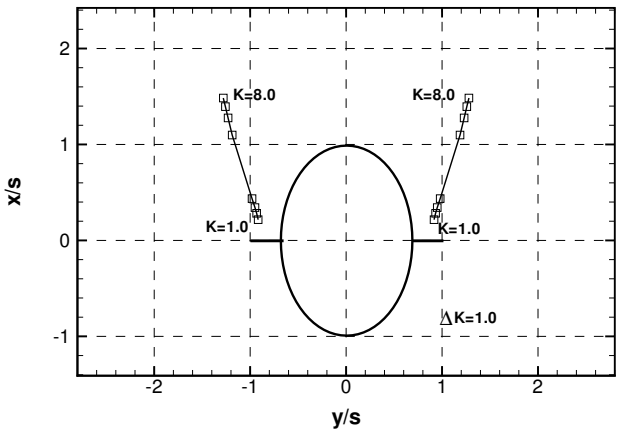

Fig. 10 Location of stationary symmetric vortex pairs over a wing-body combination of a flat-plate delta wing and an elliptic-cone body, $\gamma = b/s = 0.7$, $\tau = c/b = 1.5$, $K = 1.0 \sim 8.0$, $K_S = 0.0$.

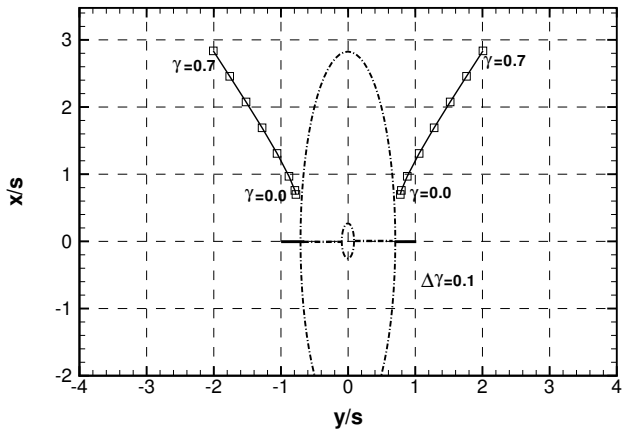

Fig. 12 Location of stationary symmetric vortex pairs over a wing-body combination of a flat-plate delta wing and an elliptic-cone body, $\gamma = b/s = 0.0 \sim 0.7$, $\tau = c/b = 4.0$, $K = 4.0$, $K_S = 0.0$.

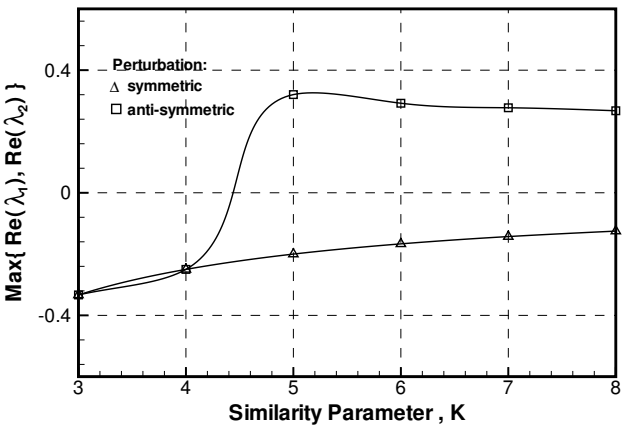

Fig. 11 Maximum real part of the eigenvalues for symmetric vortex pairs over a wing-body combination of a flat-plate delta wing and an elliptic-cone body, $\gamma = b/s = 0.7$, $\tau = c/b = 1.5$, $K = 3.0 \sim 8.0$, $K_S = 0.0$.

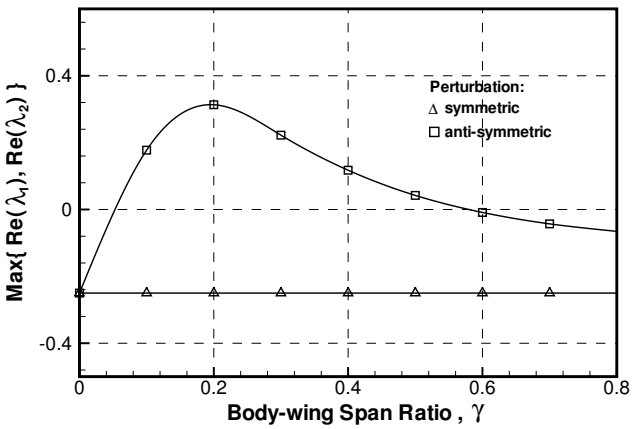

Fig. 13 Maximum real part of the eigenvalues for symmetric vortex pairs over a wing-body combination of a flat-plate delta wing and an elliptic-cone body, $\gamma = b/s = 0.0 \sim 0.7$, $\tau = c/b = 4.0$, $K = 4.0$, $K_S = 0.0$.

ratio $\tau = c/b = 4.0$. Fig. 12 shows the location of possible stationary symmetric vortex pairs at $K = 4.0$ and $\gamma = b/s$ ranging from 0.0 to 0.7. The symmetric vortex pair moves steadily upward and outboard as the body-span-to-wing-span ratio γ is increased from 0 to 0.7. Stationary asymmetric vortex solutions can be found for this case when γ is large enough.

Fig. 13 shows the eigenvalues of the vortex system vs. γ. The vortex pair is stable when $\gamma < 0.05$ or $\gamma > 0.57$ and unstable when $0.05 < \gamma < 0.57$. As γ grows up from 0, the initially stable symmetric vortex pair first becomes unstable due to the presence of the body, and then changes back to stable due to that the large height of the elliptic cone reduces the interaction of the vortex pair. This behavior is rather similar to that found in Ref. 13 for a flat-plate delta wing when vertical flat-plate fins are added along the centerline. A short fin will destabilize the symmetric vortex pair while the vortex pair becomes stable again when the fin height is increased to a critical height.

Shanks[24] in his subsonic flow measurements found that the leading edge symmetric vortices over the flat-plate delta wing with $\varepsilon = 6°$ became asymmetric at $\alpha \geq 24°$. The asymmetric moment was caused by vortex asymmetry, rather than vortex breakdown.[25] This contradicts the observations by Stahl et al.[12] (1992) where no asymmetry was found before vortex breakdown. Ericsson[26] (1992) noted, however, that

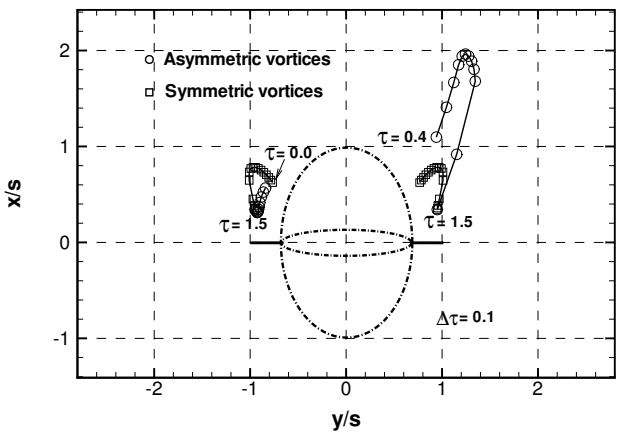

Fig. 14 Location of stationary symmetric and asymmetric vortex pairs over a wing-body combination of a flat-plate delta wing and an elliptic-cone body, $\gamma = b/s = 0.7$, $\tau = c/b = 0.0 \sim 1.5$, $K = 3.0$, $K_S = 0.0$.

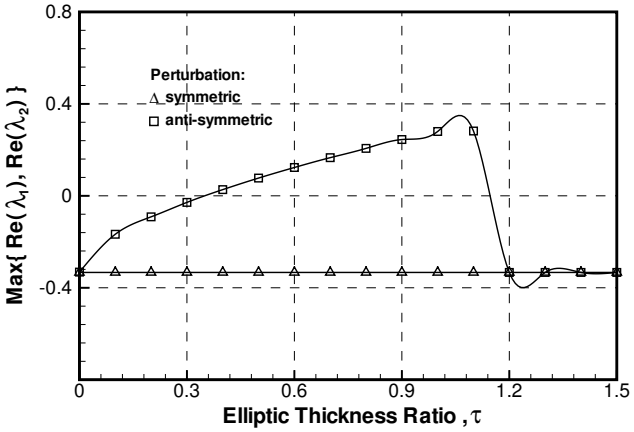

Fig. 15 Maximum real part of the eigenvalues for symmetric vortex pairs over a wing-body combination of a flat-plate delta wing and an elliptic-cone body, $\gamma = b/s = 0.7$, $K = 3.0$, $K_S = 0.0$.

Shanks' delta wing model had a 'fuselage bump' of the height $h/s = 0.5$ on the leeward side and claimed that the vortex asymmetry was not due to hydrodynamic instability but rather likely due to asymmetric reattachment in the presence of the centerline 'fuselage bump' on the leeside of the Shanks' wing model. This controversy led to the previous study by the authors[13] of the vortex stability over the delta wing with a triangular flat-plate fin in the leeside of the wing. It was concluded there that the vortex asymmetry observed in Shanks' experiment was due to the destabilizing effect of the 'short' bump, which was simulated by a short vertical flat-plate fin in Ref. 13. In the context of the present studies shown in Figs. 12 and 13, this conclusion is affirmed if the centerline 'fuselage bump' is to be approximated by the high elliptic body.

Finally, the effect of changing the body thickness-to-span ratio $\tau = c/b$ is examined. Only zero sideslip is considered. Fig. 14 shows the location of possible stationary symmetric and asymmetric vortex pairs vs. τ from 0.0 to 1.5 for fixed $\gamma = b/s = 0.7$ and $K = 3.0$. As τ increases from zero, the stationary symmetric vortex pair first moves upward and outboard until $\tau = 1$ and then move downward and inboard. No asymmetric vortex pair solutions are found when $\tau < 0.4$ and $\tau \geq 1.5$. For the stationary asymmetric vortex pair, the lower vortex moves downward and outboard. However, the upper vortex moves upward and outboard when τ increases from 0.4 to 1.0 and then downward and inboard when τ changes from 1.0 to 1.5. When $\tau = 1.5$, the asymmetric vortex pair becomes symmetric and thus coincides with the symmetric vortex pair.

Fig. 15 shows eigenvalues vs. τ for the symmetric vortex pair. The vortex pair is stable when $\tau < 0.35$

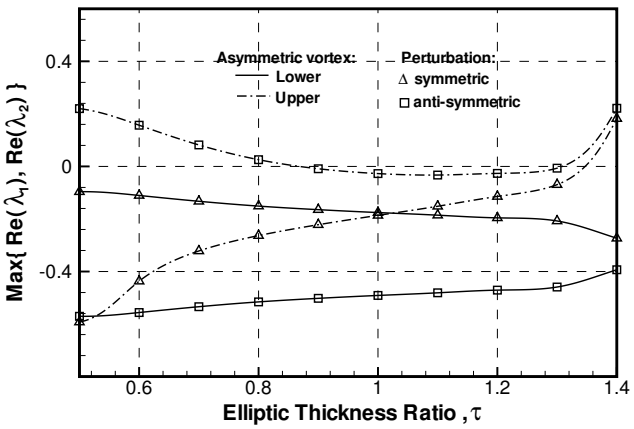

Fig. 16 Maximum real part of the eigenvalues for asymmetric vortex pairs over a wing-body combination of a flat-plate delta wing and an elliptic-cone body, $\gamma = b/s = 0.7$, $K = 3.0$, $K_S = 0.0$.

and $\tau > 1.14$ (i.e. the elliptic cone is thin or thick enough) and unstable otherwise.

Fig. 16 shows the eigenvalues vs. τ for the asymmetric vortex pairs. In the calculated region of $\tau(0.5 \sim 1.4)$, the lower vortex of a vortex pair is stable. The upper vortex is unstable when $\tau < 0.86$ or $\tau > 1.31$ and stable otherwise. Therefore, the asymmetric vortex pair as a whole is stable under small perturbation when $0.86 < \tau < 1.31$. Again, for the considered asymmetric vortices, the upper vortex is more unstable than the lower one under anti-symmetric disturbances. Note that for this case, both the symmetric and asymmetric vortex pairs are stable for $1.14 < \tau < 1.31$, and are unstable for $0.35 < \tau < 0.86$.

V. Conclusions

The stability theory developed by the present authors in Ref. 13 for vortex pairs over conical slender bodies in an inviscid, incompressible flow at high angles of attack is applied to study the stability of symmetric and asymmetric vortex pairs over flat-plate delta wing and circular cone or elliptic cone combinations. Results are compared with available experimental data. The following conclusions are drawn.

For circular-cone body and flat-plate wing combinations:

1. By adding the delta wing to the circular-cone body, the originally unstable vortex pair over the circular cone becomes stable when the wing span is large enough relative to the body radius for limited angles of attack. The stationary symmetric vortex pair changes from being stable to unstable as the cone-wing span ratio increases from zero to one, and also as the Sychev similarity parameter K increases. The present analytical results confirm the well-known effects of nose strakes in suppressing flow asymmetry about pointed slender body at high angles of attack. The analysis may be used to provide guidelines in the design of fuselage-nose strakes.

2. When K is sufficiently large or the body-span-to-wing-span ratio γ is large enough, there exists stationary asymmetric vortex pairs over the circular cone and flat-plate delta wing combination in addition to stationary symmetric vortex pairs. Such asymmetric vortex pairs may be stable. An initially stable symmetric vortex pair may transit into a stable asymmetric pair as K increases for a given configuration.

3. The unstable stationary symmetric vortex pair at zero sideslip can change to a stable asymmetric vortex pair when the sideslip similarity parameter K_S is large enough. In other words, sideslip may stabilize the originally unstable symmetric vortex pair at no sideslip.

For elliptic-cone body and flat-plate wing combinations:

1. For an ellipse thickness ratio greater than one, the stationary symmetric vortex pair changes from being stable to unstable when the body-span-to-wing-span ratio γ increases from zero, and changes back to stable when γ becomes large enough. The present analysis affirms previous findings in Ref. 13 that the flow asymmetry observed by Shanks[24] is caused by the destabilizing effect of the short leeward-side bump on his test wing model.

2. For given body-span-to-wing-span ratio and K, the stationary symmetric vortex pair changes from being stable to unstable when the ellipse thickness ratio increases from zero, and changes back to stable when the thickness ratio becomes sufficiently large. On the other hand, an asymmetric vortex pair changes from being unstable to stable when the ellipse thickness ratio increases, and then changes back to unstable when the thickness ratio becomes sufficiently greater than one.

Finally, in general, the upper vortex of an asymmetric vortex pair is more unstable than the lower vortex under anti-symmetric perturbations. There exist conditions under which no stable conical vortex flow solutions can be found over a conical wing-body combination.

References

[1]Hunt, B. L., "Asymmetric vortex forces and wakes on slender bodies," AIAA Paper 1982–1336, 1982.

[2]Ericsson, L. and Reding, J., "Asymmetric flow separation and vortex shedding on bodies of revolution," *Tactical Missile Aerodynamics: General Topics, Progress in Astronautics and Aeronautics*, edited by M. Hemsh, Vol. 141, American Institute of Aeronautics and Astronautics, New York, 1992, pp. 391–452.

[3]Champigny, P., "Side forces at high angles of atack. Why, when, how?" *La Recherche Aerospatiale*, , No. 4, 1974, pp. 269–282.

[4]Lamont, P. J., "Pressures Around an Inclined Ogive Cylinder with Laminar,Transitional,or Turbulent Separation," *AIAA Journal*, Vol. 20, No. 11, Nov. 1982, pp. 1492–1499.

[5]Zilliac, G. G., Degani, D., and Tobak, M., "Asymmetric vortices on a slender body of revolution," *AIAA Journal*, Vol. 29, 1991, pp. 667–675.

[6]Degani, D., "Effect of geometrical disturbance on vortex asymmetry," *AIAA Journal*, Vol. 29, 1991, pp. 560–566.

[7]Degani, D., "Instabilities of flows over bodies at large incidence," *AIAA Journal*, Vol. 30, 1992, pp. 94–100.

[8]Hartwich, P. M., Hall, R. M., and Hemsch, M. J., "Navier-Stokes computations of vortex asymmetries controlled by small surface imperfections," *Journal of Spacecraft and Rocket*, Vol. 28, No. 2, Mar.-Apr. 1991, pp. 258–264.

[9]Dyer, D. E., Fiddes, S. P., and Smith, J. H. B., "Asymmetric vortex formation from cones at incidence – a simple inviscid model," *Aeronautical Quarterly*, Vol. 31, 1982, pp. 293–312.

[10]Pidd, M. and Smith, J. H. B., "Asymmetric vortex flow over circular cones," *Vortex Flow Aerodynamics, AGARD CP-494*, July 1991, pp. 18–1–11.

[11]Huang, M. K. and Chow, C. Y., "Stability of leading-edge vortex pair on a slender delta wing," *AIAA Journal*, Vol. 34, 1996, pp. 1182–1187.

[12]Stahl, W., Mahmood, M., and Asghar, A., "Experimental investigations of the vortex flow on delta wings at high incidence," *AIAA Journal*, Vol. 30, 1992, pp. 1027–1032.

[13]Cai, J., Liu, F., and Luo, S., "Stability of symmetric vortices in two-dimensions and over three-dimensional slender conical bodies," *J. Fluid Mech.*, Vol. 480, 2003, pp. 65–94.

[14]Cai, J., Luo, S., and Liu, F., "Stability of Symmetric and Asymmetric Vortex Pairs over Slender Conical Wings and Bodies," AIAA Paper 2003-1101, January 2003.

[15]Jenista, J. M. and Nelson, R. C., "The influence of high angle-of-attack flow phenomena on the dynamic stability of slender missiles," Air Force Armament Lab. AFATL TR 83-04, 1983.

[16]Lowson, M. and Ponton, A., "Symmetry breaking in vortex flows on conical bodies," *AIAA Journal*, Vol. 30, 1992, pp. 1576–1583.

[17]Coe, P., Chambers, J., and Letko, W., "Asymmetric lateral-directional characteristics of pointed bodies of revolution at high angle of attack," NASA TN D-7095, 1972.

[18]Erickson, G. E. and Lorincz, D. J., "Water tunnel and wind tunnel studies of asymmetric load alleviation on a fighter aircraft at high angles of attack," AIAA Paper 1980–1618, Aug. 1980.

[19]Nelson, R. and Malcolm, G., "Visualization of high-angle-of-attack flow phenomena," *Tactical Missile Aerodynamics: General Topics, Progress in Astronautics and Aeronautics*, edited by M. Hemsh, Vol. 141, American Institute of Aeronautics and Astronautics, New York, 1992, pp. 195–250.

[20]Sychev, V., "Three-dimensional hypersonic gas flow past slender bodies at high angle of attack," *Journal of Maths and Mech. (USSR)*, Vol. 24, 1960, pp. 296–306.

[21]Rossow, V. J., "Lift enhancement by an externally trapped vortex," *Journal of Aircraft*, Vol. 15, 1978, pp. 618–625.

[22]Asghar, A., Stahl, W., and Mahmood, M., "Suppression of vortex asymmetry and side force on a circular cone," *AIAA Journal*, Vol. 32, 1994, pp. 2117–2120.

[23]Ng, T., "Effect of a single strake on the fore body vortex asymmetry," *Journal of Aircraft*, Vol. 27, 1990, pp. 844–846.

[24]Shanks, R., "Low-subsonic measurements of static and dynamic stability derivatives of six flat-plate wing having leading-edge sweep angles of 70° to 84°," NASA TN D-1822, 1963.

[25]Keener, E. and Chapman, G., "Similarity in vortex asymmetries over slender bodies and wings," *AIAA Journal*, Vol. 15, 1977, pp. 1370–1372.

[26]Ericsson, L., "Sources of high alpha vortex asymmetry at zero sideslip," *Journal of Aircraft*, Vol. 29, 1992, pp. 1086–1090.